INTEGRATED USE OF OPTICAL AND RADAR DATA FOR CROPLAND MAPPING OVER THE MOUNTAIN SLOPE AREA IN BOYOLALI, INDONESIA

Vidya Nahdhiyatul FIKRIYAH[1], Nirma Lila ANGGANI[1], Umar El Izzudin KIAT[1], Fithrothul KHIKMAH[2], Wildan Abdul ARROYAN[1] and Muh Faqih RIZKI[1]

DOI: 10.21163/GT_2023.181.08

ABSTRACT:
Mapping agricultural land cover data is important as an effort to support national food security, especially in Boyolali, Central Java Province, Indonesia which is one of the national rice granaries. However, mapping in the mountain slope area using optical data only is challenging due to cloud cover. The development of remote sensing technology has encouraged the possibility to integrate data with different sensors. This data integration is needed to optimize the ability to detect and map cropland that has a variety of characteristics. Therefore, this study aims to identify the cropland through the integration of time-series optical and Synthetic Aperture Radar (SAR) data. Detection of cropland was carried out using 2021 data. Polarisation of VV, VH, and ratio of VV/VH data was derived from the Sentinel-1, whereas image indices of Normalized Difference Vegetation Index (NDVI), Normalized Difference Water Index (NDWI), and Soil Adjusted Vegetation Index (SAVI) data were obtained from Sentinel-2. Data of Sentinel-1 and Sentinel-2 was combined and several features were selected based on their importance score. Random Forest (RF) classification was then performed. The result show that the mapping using integrated data could improve the accuracy. This indicates the possibility of data to be implemented in further studies such as the cropland type mapping and the estimation of food productivity.
Keywords: *Optical, Synthetic Aperture Radar, Integration, Cropland, Random Forests.*

1. INTRODUCTION

The need for accurate land cover data, especially cropland, cannot be separated from its important role to support strategic planning in a region. Data on where and when the cropland planted, as well as the accessibility are critical as a basis for effective measure on maintaining national food security (Susilo & Harini, 2018). Since land cover extent is dynamic, therefore, the observation should be done in a timely manner. In particular, the Indonesian government has launched the *Nawacita* program in 2015 where the national food self-sufficiency becomes one of priority targets in national development. For that reason, the accurate data on cropland is highly essential not only for national but also the global purpose as it is also mentioned in the Sustainable Development Goals (SDGs).

Remote sensing technology plays a role in extracting and monitoring land cover which is known to have variations in spectral, temporal, and spatial resolution. Remote sensing with optical sensors has been widely used for land monitoring (Gumma et al., 2019; Piao et al., 2021; Sarono et al., 2015), but the image quality and accuracy of mapping using this sensor depends on atmospheric conditions. Primarily the use of optical data is a challenge due to high cloud interference in tropical countries. To overcome these cloud problems, there is a Synthetic Aperture Radar (SAR) data which has the advantage of recording that is not affected by weather conditions. In other words, remote sensing has been developed in different specifications, so there are more approaches in land detection, such as combining optical and SAR imagery (Joshi et al., 2016).

[1]*Faculty of Geography, Universitas Muhammadiyah Surakarta, Indonesia, *Corresponding author: vidya.n.fikriyah@ums.ac.id; nla624@ums.id; uei665@ums.id; e100170108@student.ums.ac.id; e100190281@student.ums.ac.id.*
[2]*Photogrammetry and Geoinformatics, The Stuttgart Technology University of Applied Sciences, Germany, 12khfi1mpg@hft-stuttgart.de*

The complexity in agricultural area creates a challenge in mapping cropland using optical data (Fritz et al., 2015). Not only that, specifically rice crop is also cultivated in different land-climatic and ecosystems following the sequence in topography, from upland, rainfed lowland, irrigated, to flood prone area (Kuenzer & Knauer, 2012). Despite the relatively high revisit time of Sentinel-2, the observation of cropland in the cloud-prone tropical and sub-tropical area using this data only is still challenging (Singha et al., 2019). Thus, data integration with Sentinel-1 that is independent of sun illumination (Kuenzer & Knauer, 2012) is potential to help mapping cropland in such condition. Recently, the combination of optical and SAR data crop has been employed in the subtropical area using backscatter from Sentinel-1 and NDVI from Sentinel-2 data (Cai et al., 2019). Also, observation of paddy field in the tropical lowland coastal area has also been conducted using Sentinel-1 and 30-m resolution of Landsat data (Arjasakusuma et al., 2020), making a limitation in capturing smallholder fields. In this context, to date the ability of integration Sentinel-2 and Sentinel-1 to map cropland in a tropical mountain slope region has not been given much attention.

Furthermore, in the last decade, the use of machine learning algorithms for remote sensing has received a lot of attention. The application is mainly related to the study of land cover/use classification. Algorithms commonly used to date include support vector machines (SVM), decision trees, random forests (RF), and convolutional neural networks (CNN) (Sheykhmousa et al., 2020). These methods have advantages in terms of complex pattern retrieval capabilities and informative features of remote sensing satellite imagery. In this case, Random Forest (RF) was implemented for classification as it is known to improve the classification accuracy for time-series data without overfitting problem (Piao et al., 2021).

Given the above background, the general objective of this study is to map cropland based on the integration of optical and SAR time-series data. In addition, to capture the timely or seasonal spectral variability of different land cover, the multi-temporal remote sensing data is required. Feature selection will be performed to choose the most informative inputs for classification and RF classifier would be implemented for mapping. Then, a comparison of accuracy would be conducted among classification results using Sentinel-1, Sentinel-2, and the integration of them.

2. STUDY AREA AND DATA

2.1. Study area

The study was carried out in Regency of Boyolali, Province of Central Java, Indonesia. According to the department of regional statistic (BPS Boyolali, 2021), rice crop is the dominant crop in Boyolali (**Fig.1**) and its harvesting area reached 47,760.01 hectares with a total production of 225,425.92 ton in 2020. This makes the regency becomes the ninth largest rice producer in Central Java. Boyolali is situated in the slope area of two volcanos, the Mount Merapi (2,910 m) and Merbabu (3,145 m) in the western side (**Fig.2**). The elevation varies between 75-1,500 msl.

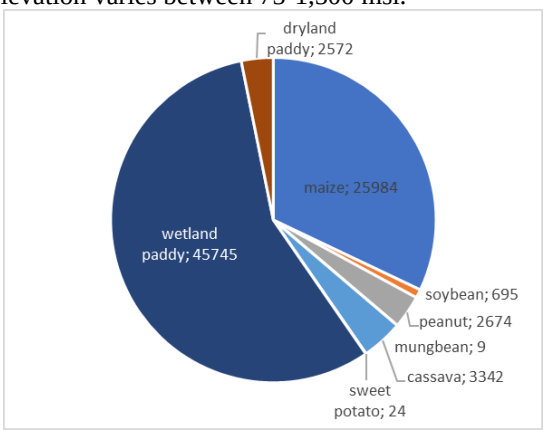

Fig. 1. Harvested area (hectares) of different crop in Boyolali in 2019 (*Source: Regional statistics, 2020*).

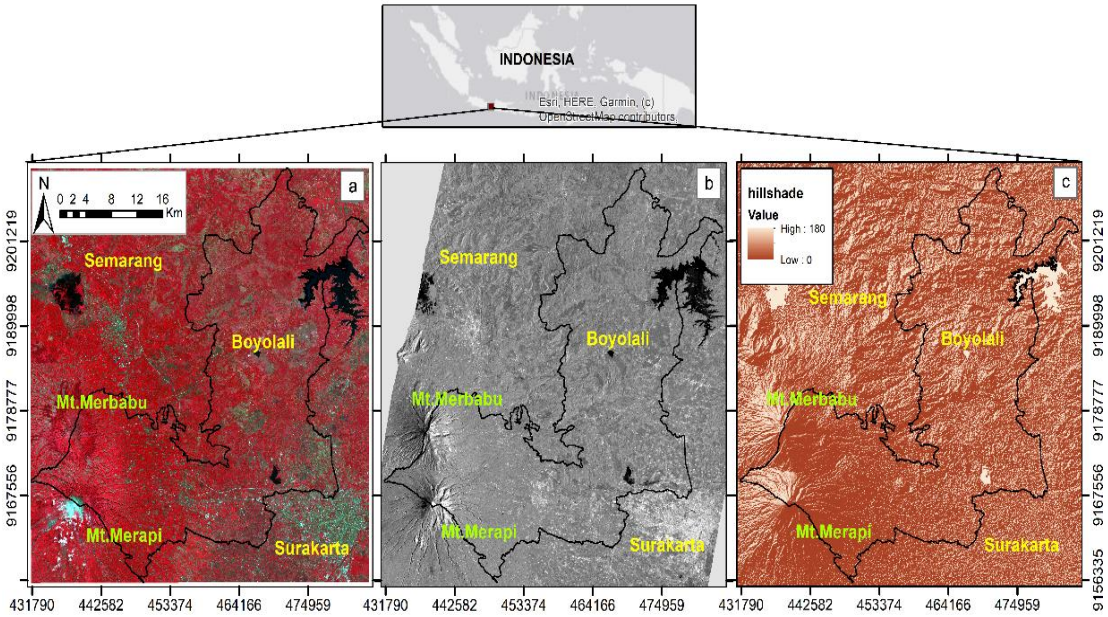

Fig. 2. Location of Boyolali, Indonesia shown in: a) Sentinel-2 data (RGB composite using NIR, red, and green band, respectively); b) Sentinel-1 VV data; and c) Hillshade from ASTER GDEM data.

2.2. Synthetic Aperture Radar (SAR) data collection and processing

One of the products of the Sentinel satellite project is Sentinel-1. It uses a C-band SAR sensor where object identification is based on backscatter. In this study, Sentinel-1 time-series data will be used to extract backscattering of land cover classes. The data selected is Sentinel-1A Level 1 Ground Range Detected (GRD) with dual polarisation (VV and VH) which was downloaded from https://scihub.copernicus.eu/dhus/#/home. The data acquisition period is April, July, and August 2021, taking into account a whole cropping season from rice crop calendar since it is the dominant crop in the study area (**Fig.1**). The characteristics of data used in the study is presented in **Table 1**.

Table 1.

Specifications of Sentinel-1 data used in the study.

Satellite	Sentinel-1A
Height/inclination	693 km/98.18º
Wavelength	C-band (3.75 – 7.5 cm)/ 5.405 GHz
Polarisation	VV+VH
Pixel spacing	10 m
Acquisition date	April, July, and August 2021

GRD product is Sentinel-1A data that has been calibrated radiometrically. The next step is the use of Refined Lee filters to remove speckle effects (Argenti et al., 2013). A geometric correction was done through the Sentinel application platform (SNAP) program, which is a software developed by European Space Agency (ESA). For this purpose, the Shuttle Radar Topography Mission (SRTM) 1 arc-second resolution data was used directly in SNAP. Finally, the image is then cropped using the Boyolali administrative boundary from the Global Administrative Area (GADM). Then, three datasets of polarisations were produced (VV, VH, and ratio of VV/VH) to explore the spectral variations of land covers.

2.3. Optical data collection and processing

Sentinel-2 level 2A was used as the optical data. This data has been corrected radiometrically and geometrically, as its numbers represent the reflectance at the Bottom of Atmosphere (BOA) level so that it can be used immediately. We applied the function to collect monthly composite image in Google Earth Engine (GEE) environment following steps in https://developers.google.com/earth-engine/datasets/catalog/COPERNICUS_S2_SR. Median function was used for the composite image.

To filter cloudy scenes, a maximum cloud percentage of 30% was set as the limit because no good image is available below that. The time-series images were then cropped based on the administrative coverage of Boyolali Regency using administrative data from GADM. Specifications of data used for the study is presented in **Table 2**.

Table 2.

Specifications of Sentinel-2 data used in the study.

Satellite	**Sentinel-2A**
Wavelength (spatial resolution)	Band 3, 4, and 8 for Green, Red, and NIR respectively (10 m)
Level	Level-2A
Acquisition date	April, July, and August 2021

3. METHODS

3.1. Image Indices

In the next step after the pre-processing of Sentinel-2 data, three vegetation indices were produced. Those vegetation index algorithms were used for the RF classification input. Sentinel-2 images were processed and its pixel values were transformed into Normalized Difference Vegetation Index (NDVI), Normalized Difference Water Index (NDWI), and Soil Adjusted Vegetation Index (SAVI) as stated in formula 1-3. NDVI is one of the most commonly used for vegetation studies, while SAVI has capability to minimize the effect of soil brightness (Sashikkumar et al., 2017). In addition, NDWI is sensitive to the moisture of plants and soil enabling better discrimination between crop and surface water body (Bhattacharya et al., 2021).

$$NDVI = \frac{NIR - Red}{NIR + Red} \quad (1)$$

$$NDWI = \frac{Green - NIR}{Green + NIR} \quad (2)$$

$$SAVI = \frac{NIR - Red}{NIR + Red + L} * (1 + L) \quad (3)$$

where, NIR, Red, and Green is the pixel values for each band, respectively, and L is the soil adjustment factor (0.5). SAVI was used to normalize the subtractive soil variations by applying an adjustment factor (L) to reduce the soil background variations. The L values were adjusted lower as vegetation cover increased (Mostafiz et al., 2021). L value 0.5 was used in this study, considering the medium levels of vegetation cover in the whole area and for crop detection.

3.2. Image classification process

For this study, three RF classification schemes of multi-temporal data were conducted using (1) image indices (NDVI, NDWI, and SAVI) from Sentinel-2 dataset only, (2) VV, VH, and ratio of VV/VH dataset only, and (3) the integration of the first and second dataset. There were five classification classes used, namely cropland, built-up, water body, bare land, and forest. Plots of all classes were visually identified using a high-resolution imagery in Google Earth Pro. In total, 100 plots were taken for each built-up, forest, and cropland class, whereas, 50 plots were identified for

each water body and bare land. Plots were then divided into 70% for the training data in RF classification and 30% for the accuracy measurement test. **Fig. 3** shows the distribution of training and validation plots.

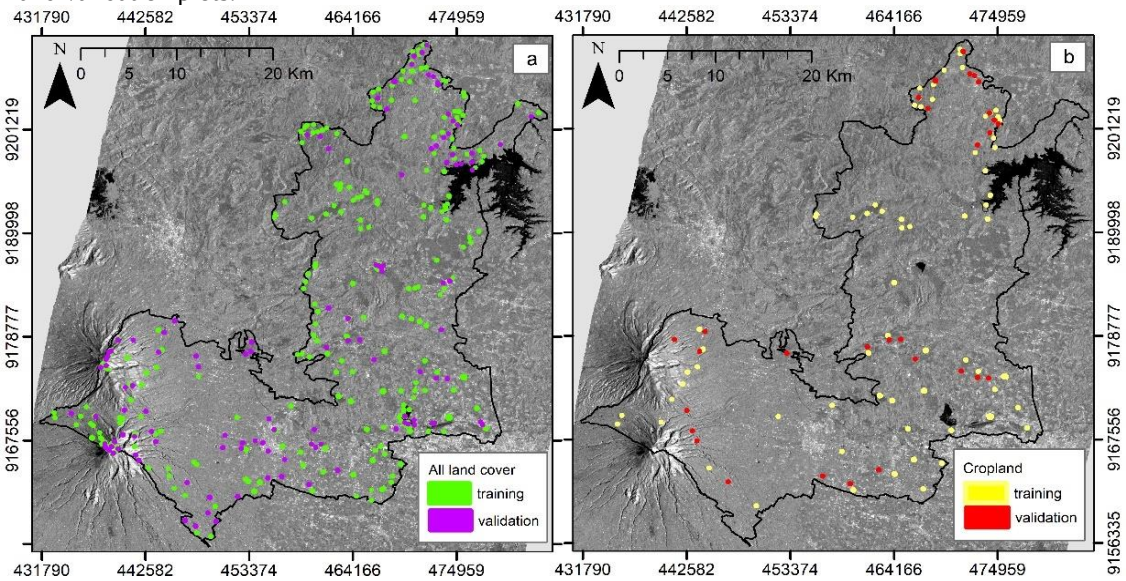

Fig. 3. Plots distribution for a) all land cover types and b) cropland only.

After creating a stack containing Sentinel-1 and 2 images, we calculated the variable importance to assess the relevant inputs for random forest classification.Variable importance scores were calculated based on Gini coefficient in ArcGIS Pro 2.9.0. The number indicates the frequency of a variable is responsible for a split in the model Feature selection entails the most informative features to reduce the effect of high-dimensional data (Akbari et al., 2020). In the RF classification, the maximum *ntree* was set at 50, maximum number tree depth was 30 and maximum number of samples per class was 1000. Converged color and mean digital number were included as the segment attributes. The overview of all steps taken in this study is presented in **Fig. 4**.

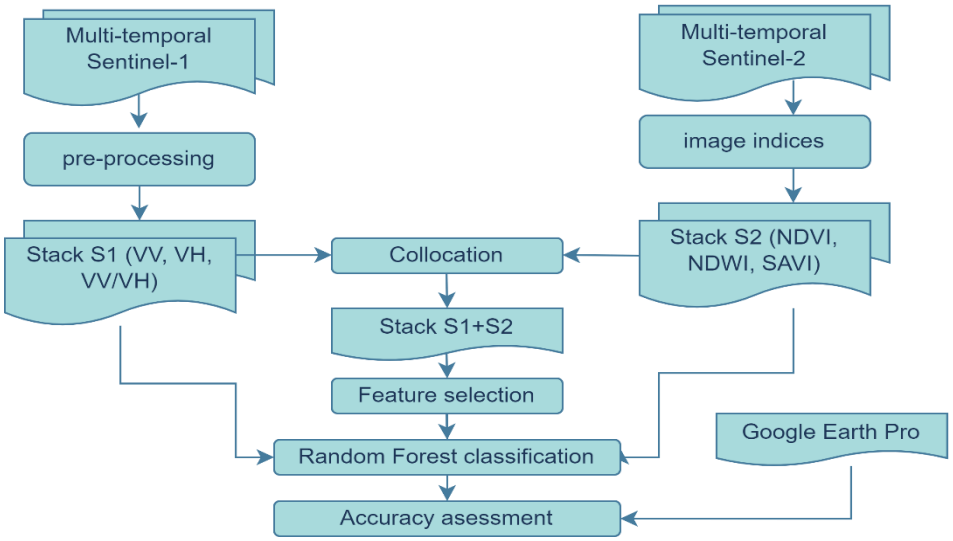

Fig. 4. Steps on the integration of Sentinel-1 and 2 data.

4. RESULTS

4.1. Key Classification in Sentinel-1

The result of pre-processing Sentinel-1 data is as follows. **Fig.5** shows the appearance of built-up, forest, water body, cropland, and bare land observed through Sentinel-1 (VV, VH, and the RGB composite). From the figure, it can be seen that every land cover has distinct characteristics of SAR backscatters. Built-up area gives brighter pixels compared to water body and bare land area. This indicates the higher level of backscatter from built-up area caused by the double bounce and corner reflectance (Deepthi et al., 2018). Meanwhile, the forest and cropland areas were identified having more colour variations in the pixels. In comparison to the cropland, forest areas however, have a slightly brighter tone as their dominant scattering mechanism are from the volume scattering related to the higher biomass in canopies and the double- bounce effect from the vertical trunk structure (Ningthoujam et al., 2016).

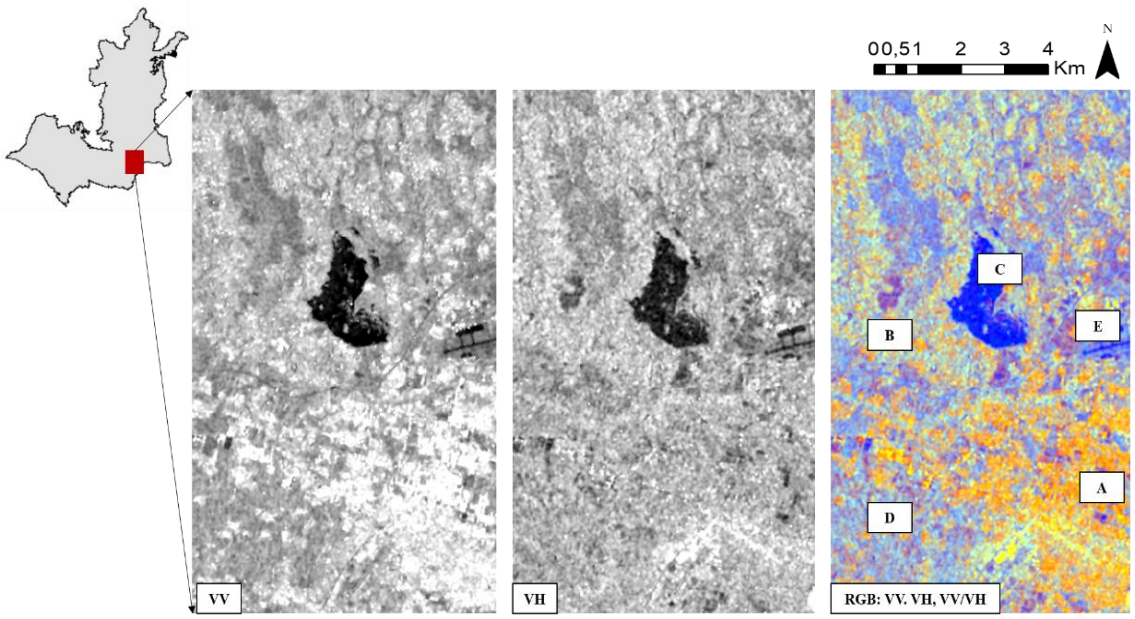

Fig. 5. Visual key interpretation of Sentinel-1 (VV, VH, and RGB composite VV, VH, VV/VH) data, showing A: built-up, B: forest, C: water body, D: cropland, and E: bare land.

Since a time-series data was used, the temporal variation of each land cover class can be observed in **Fig. 6**. The figure shows that cropland has a backscattering pattern that is different from other land covers. This change in backscattering is related to the growth phase of crop (Nguyen & Wagner, 2017). Built-up areas have the highest backscatter and relatively constant throughout the period, while water bodies remain giving the lowest backscatter response among other classes.

The classification results in **Table 3** shows that the classification accuracy of using Sentinel-1 data, giving the overall accuracy of 78%. For the user's accuracy, the value of bare land, cropland, and water body were high (100%, 88.46%, 83.33%, respectively). Meanwhile, high producer's classification accuracies were identified for the class of water body (100%), forest (80%), and built-up area (70%). The result suggests that high accuracy is gained for the stable class such as water body (Piao et al., 2021).

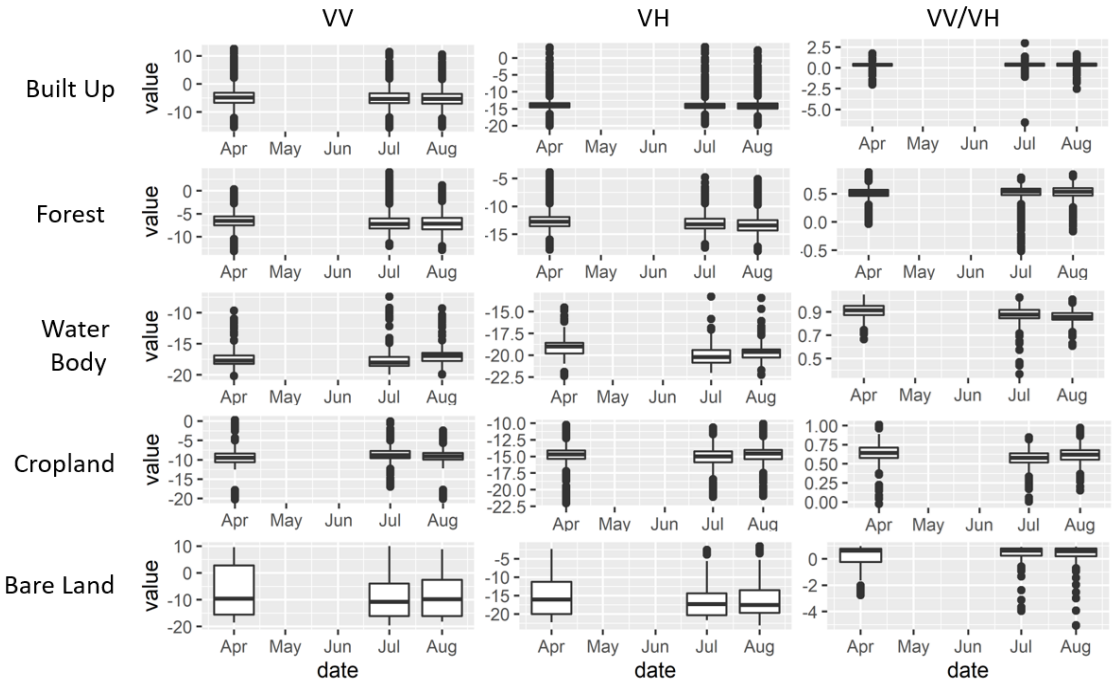

Fig. 6. Value dispersion of training data of every land cover class on VV, VH, and ratio VV/VH data.

Table 3.

Confussion matrix based on Sentinel-1.

Sentinel-1		Reference data					
		Built Up	**Forest**	**Water Body**	**Cropland**	**Bare Land**	**UA**
Classified data	Built Up	21	5	0	4	1	67.74
	Forest	8	24	0	3	0	68.57
	Water Body	0	0	15	0	3	83.33
	Cropland	1	1	0	23	1	88.46
	Bare Land	0	0	0	0	10	100.00
	PA	70.00	80.00	100.00	76.67	66.67	
Overall Accuracy		**78%**					

4.2. Spectral Indices from Sentinel-2

Fig. 7 presents the results of NDVI, NDWI, and SAVI over the study area. As shown in the figure, the distribution value of each index varied during the observation period. Overall, in April, the area was dominated by the high NDVI and SAVI value, especially in the northern part of region. This means that there was a high level of greenness on that period as the rainy season occur. In July, when the dry season occurred, most part of the region were in the middle and low value of all indices. High NDVI and SAVI value, however, were seen in the southwestern part where top of Mount Merapi and Merbabu located (**Fig.2**). For the last observation period, almost all areas were covered by the moderate and low value of NDVI, NDWI, and SAVI. The dryness condition in particular can be detected in the northern part of Boyolali. These value differences could be caused by different planting cycles of crop.

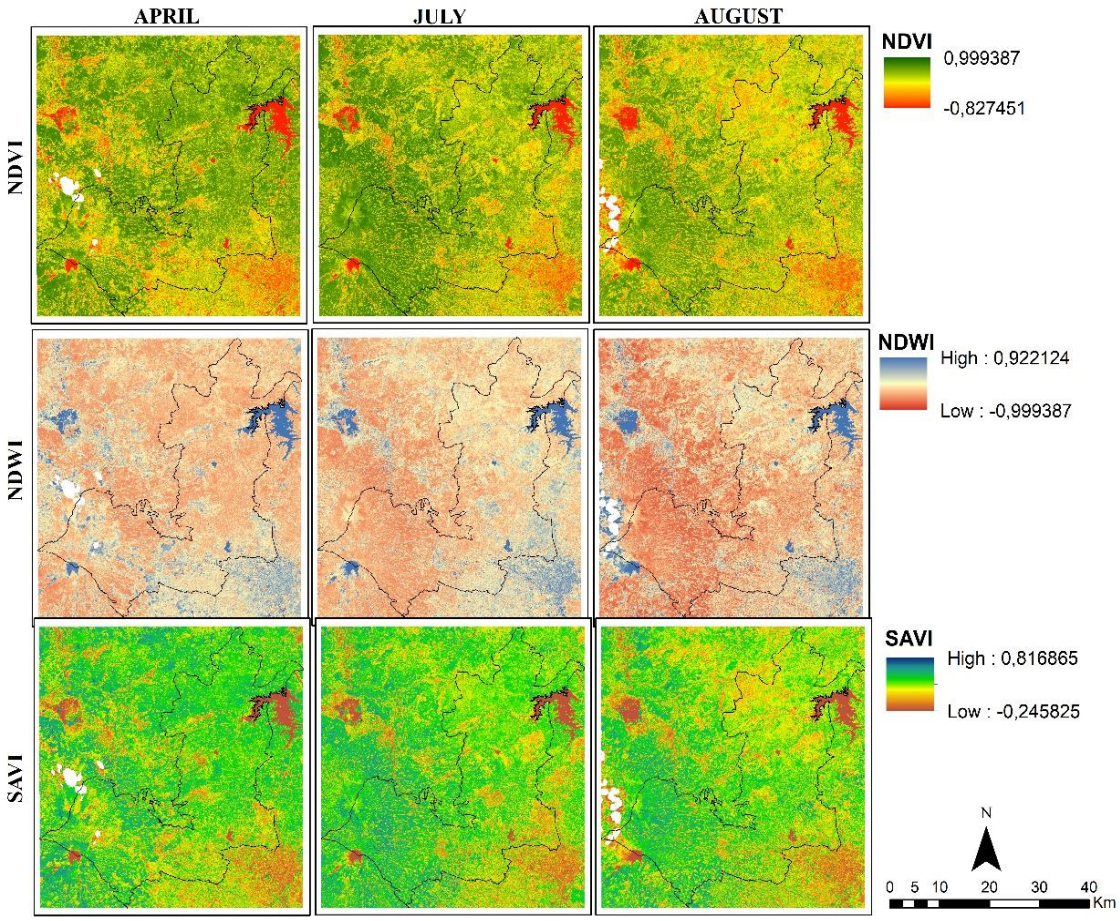

Fig. 7. NDVI, NDWI, and SAVI distribution over the study area in April, July, and August 2021.

Based on the statistical distribution of indices values (**Fig.8**), NDVI and SAVI values of the cropland showed similar ranges of value in the three months of observation. The best result of cropland classification was in August, with the shortest-range value. The median was similar to April's result, while July had the highest range and the lowest median. Built-up and water bodies were well defined in the three-month observations shown by the short range and similar median of NDVI and SAVI value. Forest was better in April and July results because the ranges of values increased in August. Bare land had a similar median value in the three months, but the distribution values varied in several parts of the area.

Furthermore, **Table 4** gives information on the classification accuracy derived from Sentinel-2 only dataset. In general, the classification produced an overall accuracy of 89% which was higher compared to the result of Sentinel-1 dataset (**Table 3**). Bare land and forest gave the highest values with 100% of user's accuracy, whereas built-up and water body area had 100% of producer's accuracy. For the cropland, it produced a user's and producer's accuracy of 89.66% and 83.87, respectively. In our findings, the use of vegetation indices increased the detection accuracy, supporting outcomes from earlier study (Panda et al., 2010). SAVI, in particular, reduces the noise of classification resulting from the soils and the moisture influences of the output (Panda et al., 2010). In this case, soil background influences the spectra of partially vegetated canopies, therefore, vegetation indices are required.

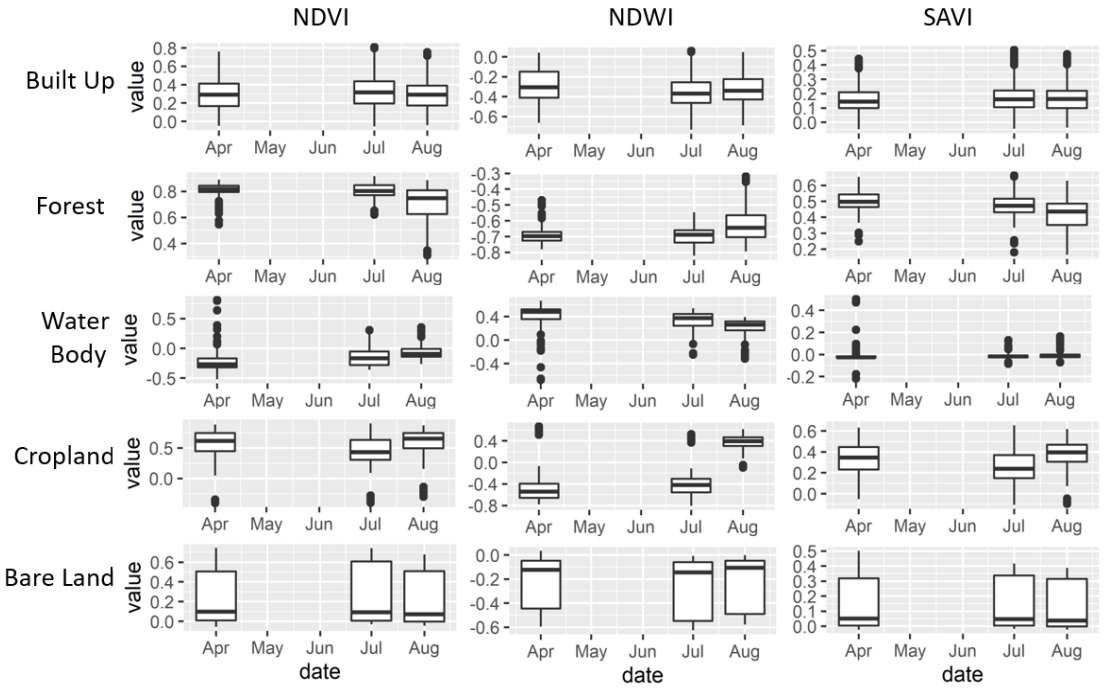

Fig. 8. Value distribution of NDVI, NDWI, and SAVI data for every land cover class.

Table 4.

Confussion matrix based on Sentinel-2.

Sentinel-2		Reference data					
		Built Up	**Forest**	**Water Body**	**Cropland**	**Bare Land**	**UA**
Classified data	Built Up	30	1	0	3	4	78.95
	Forest	0	26	0	2	0	92.86
	Water Body	0	0	15	0	0	100.00
	Cropland	0	2	0	26	1	89.66
	Bare Land	0	0	0	0	10	100.00
	PA	100.00	89.66	100.00	83.87	66.67	
Overall Accuracy		**89%**					

4.3. Cropland Area Distribution

The importance degree of variables used in RF classification is presented in **Fig.9**.

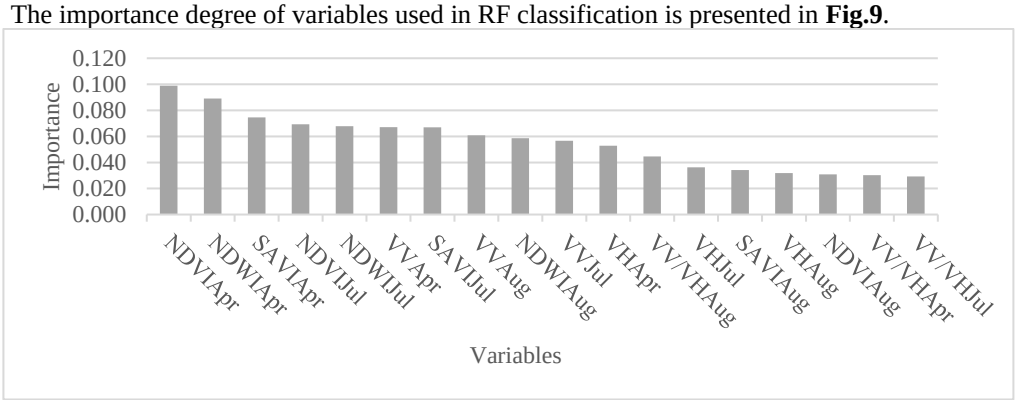

Fig. 9. Value of variable importance in Random Forest classifier.

It is shown that NDVI had the highest score among other 17 variables, followed by NDWI, and SAVI. In the first to ninth position, the high score was dominated by NDVI, NDWI, SAVI, and VV polarisation. From this finding, therefore, we selected those four variables as inputs for RF classification.

Fig.10 and **Fig.11** shows the actual condition of cropland plots in different characteristics of study area. In **Fig.10**, croplands in the upper slope of Mount Merapi and Merbabu are presented, showing the planted crops are dominated with a non-rice crop, such as vegetables and cassava. Meanwhile, the croplands located in the lower slope are shown in **Fig.11**. Croplands near to the water body were characterized by the irrigated rice field, as the high access and availability of water regardless the season (**Fig.11a**), whereas dry croplands were more prominent in the high populated urban area (**Fig. 11b**). Rice fields were also detected in the less populated urban area (**Fig. 11c**). The observed conditions from both figures, we can see that the croplands are attributed to the physical conditions, for example the topography, water, and agroecology characteristic (Widiyanto, 2019).

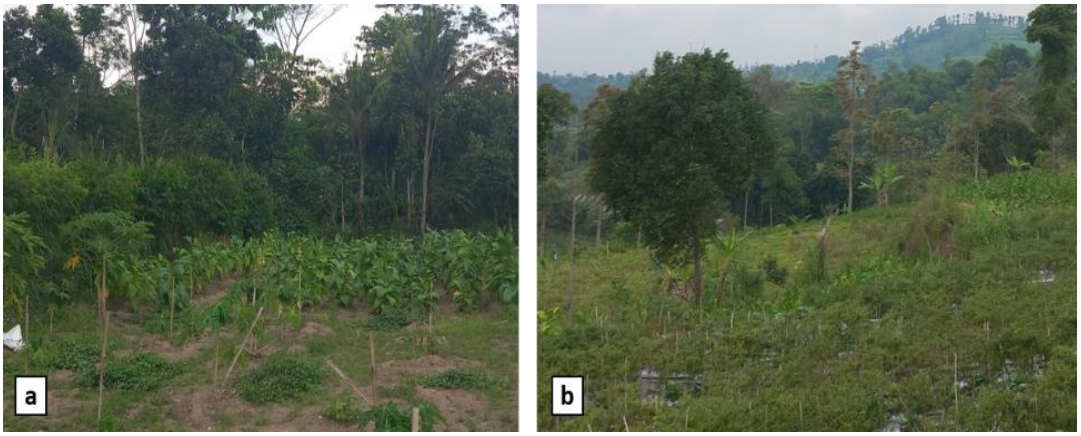

Fig. 10. Croplands condition in the upper slope of study area taken in August 2022.

Fig. 11. Cropland areas taken in August 2022. Characteristics: (a) near to water body, (b) in high populated urban region, and (c) in less populated urban region.

Implementation of RF classification with Sentinel-1 and Sentinel-2 dataset resulted a land cover map for Boyolali Regency (**Fig.12**) with an overall accuracy of 89% (**Table 5**). Cropland specifically, gained user's and producer's accuracy of 80% and 93.33%, respectively. Looking at the correct classified plots, this accuracy is higher in comparison to the previous scenarios using Sentinel-1 and Sentinel-2 alone for the input. Similarly, with RF method, a high classification accuracy was yielded for cropland mapping conducted by (Phalke et al., 2020).

Table 5.

Confussion matrix based on Sentinel-1 and 2.

Sentinel-1 and 2		Reference data					
		Built Up	**Forest**	**Water Body**	**Cropland**	**Bare Land**	**UA**
Classified data	Built Up	28	0	0	1	4	84.85
	Forest	0	27	0	1	0	96.43
	Water Body	0	0	15	0	0	100.00
	Cropland	2	3	0	28	2	80.00
	Bare Land	0	0	0	0	9	100.00
	PA	93.33	90.00	100.00	93.33	60.00	
Overall Accuracy		**89%**					

From **Fig.12**, it can be seen that dense built-up areas were in southern part of regency where the government officials are located. Water bodies, on the other hand, were only located at certain points and not evenly distributed. This condition may bring influences on the cropland characteristic based on the water use (irrigated and rainfed field) over the area.

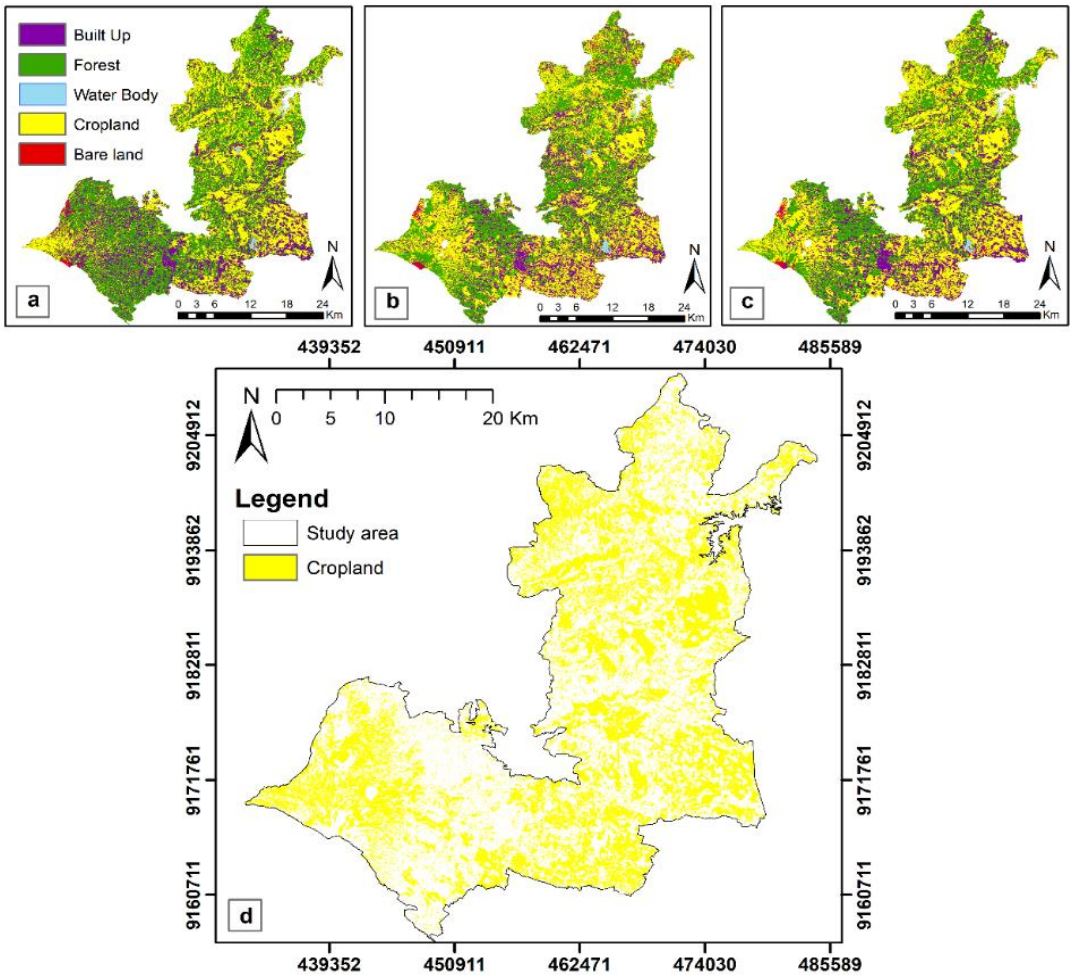

Fig. 12. Land covers from a) Sentinel-1; b) Sentinel-2; c) Sentinel-1 and -2. Figure d showing the cropland distribution based on Sentinel-1 and -2 data.

5. DISCUSSION

In this study, a different approach of mapping cropland area was taken. An integrated of optical data from Sentinel-2 and SAR data from Sentinel-1 was conducted to improve the accuracy of mapping. Based on our observation, we found that the integration of time-series optical and SAR data improved the capability of cropland detection. The proposed approach enables the combination of advantages form each data. Optical sensor of Sentinel-2 uses NIR, and green band that highlight the reflectance of vegetation. Additionally, implementation of vegetation indices also suppresses the influence of soil spectra in red band. On the other hand, Sentinel-1 with SAR sensor is beneficial for the observation in area with high cloud cover as in the mountainous area. The use of different polarisation, its combination, and the textural features could enhance the capability of identification for each land cover class (Haris et al., 2021; Priyono et al., 2022; Qi et al., 2012).

Based on our results, although there was no difference in overall accuracy between data of Sentinel-2 alone and the integration of Sentinel-1 and -2, the correct classified pixels for cropland and its PA were higher when using the integrated data. This implies the effectiveness of selected inputs performance for distinguishing cropland from other classes. Applying feature selection process, therefore, is still worth to do as it provided improvement in the accuracy of cropland detection. According to our findings, the evaluation of relative variable importance showed that all of image indices (NDVI, NDWI, and SAVI) from Sentinel-2 had the high contribution to the classification. The superior importance of NDVI was encouraging the demonstration of this index applied for mapping in a complex cropland region (Estel et al., 2016) and in a smallholder agricultural landscape (Rufin et al., 2022). In addition, only VV backscatter appeared more contributing than other variables from Sentinel-1 data. It is mainly due to VV better separability performance in discriminating water and bare land classes (el Mortaji et al., 2022) as similar finding was also reported by (Abdikan et al., 2016). The present results support the previous observation by Koley & Chockalingam (2022) that using SAR data alone is not sufficient for cropland mapping, despite its wide applications in mapping rice crop specifically because the distinct soil moisture condition in the start of crop growing season (Kuenzer & Knauer, 2012).

For future work, the use of this approach for mapping different cropland type is encouraged to fully understand the temporal, spectral, and spatial dynamic of each crop. Since our study lack information of crop type, this might contribute to the misclassification in the cropland. Apart from that, study on cropland mapping and monitoring is essential in regards to the food security matter. In fact, specifically in the study area from 2017 to 2019, its harvested area has decreased (**Fig. 13**). If the proportion of built-up that surrounds cropland is large and there is no policy preventing it, then this will affect crop productivity and further damage the food security. Findings on this study approach, therefore, could be beneficial for the improvement of cropland data accuracy supporting the regional planning policy.

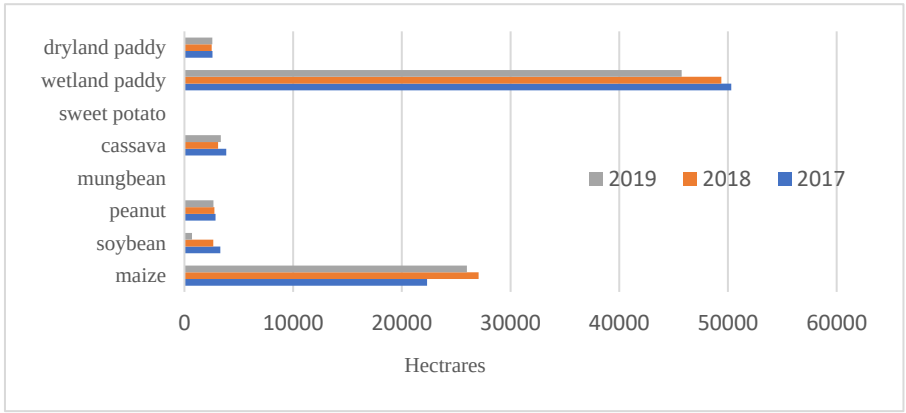

Fig. 13. Crop harvested area (in hectares) in Boyolali Regency from 2017 to 2019 (*Source: Regional statistic, 2018-2020*).

6. CONCLUSIONS

We demonstrated a different approach of mapping cropland area through an integrated of optical data from Sentinel-2 and Synthetic Aperture Radar (SAR) data from Sentinel-1. This particular approach was implemented in the mountainous slope area where generally high cloud cover occurs. Feature selection was also performed resulting NDVI, NDWI, SAVI, and VV polarization as the high importance variables. According to the results, random forest as a machine learning-based classifier could give overall accuracy of 78%, 89%, and 89% from Sentinel-1, Sentinel-2, and the combined data, respectively. Although the same overall accuracy between Sentinel-2 and combined data, the results show that the combination of optical and SAR data could increase the producer accuracy. Therefore, the results of the comparison show that the approach allow an improvement of cropland detection across the different slope area.

ACKNOWLEDGEMENTS

We would like to thank European Space Agency for providing Sentinel-1 and Sentinel-2 data freely. The authors also would like to thank to Universitas Muhammadiyah Surakarta (UMS). This work is supported by UMS under the grant scheme of 'Hibah Intergrasi Tridharma' (HIT) Number 192/A.3-III/FG/I/2022. We give a high appreciation to Department of Agriculture in Boyolali for providing insight of agriculture condition in the study area.

R E F E R E N C E S

Abdikan, S., Sanli, F. B., Ustuner, M., & Calò, F. (2016). LAND COVER MAPPING USING SENTINEL-1 SAR DATA. *The International Archives of the Photogrammetry, Remote Sensing and Spatial Information Sciences*, *XLI-B7*, 757–761. https://doi.org/10.5194/ISPRS-ARCHIVES-XLI-B7-757-2016

Akbari, E., Boloorani, A. D., Samany, N. N., Hamzeh, S., Soufizadeh, S., & Pignatti, S. (2020). Crop Mapping Using Random Forest and Particle Swarm Optimization based on Multi-Temporal Sentinel-2. *Remote Sensing 2020, Vol. 12, Page 1449*, *12*(9), 1449. https://doi.org/10.3390/RS12091449

Argenti, F., Lapini, A., Alparone, L., & Bianchi, T. (2013). A tutorial on speckle reduction in synthetic aperture radar images. *IEEE Geoscience and Remote Sensing Magazine*, *1*(3), 6–35. https://doi.org/10.1109/MGRS.2013.2277512

Arjasakusuma, S., Kusuma, S. S., Rafif, R., Saringatin, S., & Wicaksono, P. (2020). Combination of Landsat 8 OLI and Sentinel-1 SAR Time-Series Data for Mapping Paddy Fields in Parts of West and Central Java Provinces, Indonesia. *ISPRS International Journal of Geo-Information 2020, Vol. 9, Page 663*, *9*(11), 663. https://doi.org/10.3390/IJGI9110663

Bhattacharya, S., Halder, S., Nag, S., Roy, P. K., & Roy, M. B. (2021). Assessment of Drought Using Multi-parameter Indices. *Lecture Notes in Civil Engineering*, *131 LNCE*, 243–255. https://doi.org/10.1007/978-981-33-6412-7_18/FIGURES/9

BPS Boyolali. (2021). *Harvesting Area and Rice Production in Boyolali*. Badan Pusat Statistik Boyolali.

Cai, Y., Lin, H., & Zhang, M. (2019). Mapping paddy rice by the object-based random forest method using time series Sentinel-1/Sentinel-2 data. *Advances in Space Research*, *64*(11), 2233–2244. https://doi.org/10.1016/J.ASR.2019.08.042.

Deepthi, R., Ravindranath, S., & Raj, K. G. (2018). Extraction of Urban Footprint of Bengaluru City Using Microwave Remote Sensing. *The International Archives of the Photogrammetry, Remote Sensing and Spatial Information Sciences*, *XLII–5*(November), 735–740. https://doi.org/10.5194/isprs-archives-xlii-5-735-2018

el Mortaji, N., Wahbi, M., Kazzi, M. A., Alaoui, O. Y., Boulaassal, H., Maatouk, M., Zaghloul, M. N., & el Kharki, O. (2022). High Resolution Land Cover Mapping and Crop Classification in the Loukkos Watershed (Northern Morocco): An Approach Using SAR Sentinel-1 Time Series. *Revista de Teledetección*, *2022*(60), 47–69. https://doi.org/10.4995/RAET.2022.17426

Estel, S., Kuemmerle, T., Levers, C., Baumann, M., & Hostert, P. (2016). Mapping cropland-use intensity across Europe using MODIS NDVI time series. *Environmental Research Letters*, *11*(2), 024015. https://doi.org/10.1088/1748-9326/11/2/024015

Fritz, S., See, L., Mccallum, I., You, L., Bun, A., Moltchanova, E., Duerauer, M., Albrecht, F., Schill, C., Perger, C., Havlik, P., Mosnier, A., Thornton, P., Wood-Sichra, U., Herrero, M., Becker-Reshef, I., Justice, C., Hansen, M., Gong, P., … Obersteiner, M. (2015). Mapping global cropland and field size. *Global Change Biology*, *21*(5), 1980–1992. https://doi.org/10.1111/GCB.12838

Gumma, M. K., Thenkabail, P. S., Teluguntla, P. G., Oliphant, A., Xiong, J., Giri, C., Pyla, V., Dixit, S., & Whitbread, A. M. (2019). Agricultural cropland extent and areas of South Asia derived using Landsat satellite 30-m time-series big-data using random forest machine learning algorithms on the Google Earth Engine cloud. *Https://Doi.Org/10.1080/15481603.2019.1690780*, *57*(3), 302–322. https://doi.org/10.1080/15481603.2019.1690780

Haris, N. A., Kusuma, S. S., Arjasakusuma, S., & Wicaksono, P. (2021). Comparison of sentinel-2 and multitemporal sentinel-1 sar imagery for mapping aquaculture pond distribution in the coastal region of brebes regency, central java, Indonesia. *Geographia Technica*, *16*(Special Issue), 128–137. https://doi.org/10.21163/GT_2021.163.10

Joshi, N., Baumann, M., Ehammer, A., Fensholt, R., Grogan, K., Hostert, P., Jepsen, M. R., Kuemmerle, T., Meyfroidt, P., Mitchard, E. T. A., Reiche, J., Ryan, C. M., & Waske, B. (2016). A Review of the Application of Optical and Radar Remote Sensing Data Fusion to Land Use Mapping and Monitoring. *Remote Sensing 2016, Vol. 8, Page 70*, *8*(1), 70. https://doi.org/10.3390/RS8010070

Koley, S., & Chockalingam, J. (2022). Sentinel 1 and Sentinel 2 for cropland mapping with special emphasis on the usability of textural and vegetation indices. *Advances in Space Research*, *69*(4), 1768–1785. https://doi.org/10.1016/J.ASR.2021.10.020

Kuenzer, C., & Knauer, K. (2012). Remote sensing of rice crop areas. *Http://Dx.Doi.Org/10.1080/01431161.2012.738946*, *34*(6), 2101–2139. https://doi.org/10.1080/01431161.2012.738946

Mostafiz, R. B., Noguchi, R., & Ahamed, T. (2021). Agricultural Land Suitability Assessment Using Satellite Remote Sensing-Derived Soil-Vegetation Indices. *Land 2021, Vol. 10, Page 223*, *10*(2), 223. https://doi.org/10.3390/LAND10020223

Nguyen, D. B., & Wagner, W. (2017). European Rice Cropland Mapping with Sentinel-1 Data: The Mediterranean Region Case Study. *Water 2017, Vol. 9, Page 392*, *9*(6), 392. https://doi.org/10.3390/W9060392

Ningthoujam, R. K., Balzter, H., Tansey, K., Morrison, K., Johnson, S. C. M., Gerard, F., George, C., Malhi, Y., Burbidge, G., Doody, S., Veck, N., Llewellyn, G. M., Blythe, T., Rodriguez-Veiga, P., van Beijma, S., Spies, B., Barnes, C., Padilla-Parellada, M., Wheeler, J. E. M., … Bermejo, J. P. (2016). Airborne S-Band SAR for Forest Biophysical Retrieval in Temperate

Mixed Forests of the UK. *Remote Sensing 2016, Vol. 8, Page 609*, *8*(7), 609. https://doi.org/10.3390/RS8070609

Panda, S. S., Ames, D. P., & Panigrahi, S. (2010). Application of Vegetation Indices for Agricultural Crop Yield Prediction Using Neural Network Techniques. *Remote Sensing 2010, Vol. 2, Pages 673-696*, *2*(3), 673–696. https://doi.org/10.3390/RS2030673

Phalke, A. R., & Özdoğan, M. (2018). Large area cropland extent mapping with Landsat data and a generalized classifier. *Remote Sensing of Environment*, *219*, 180–195. https://doi.org/10.1016/J.RSE.2018.09.025

Phalke, A. R., Özdoğan, M., Thenkabail, P. S., Erickson, T., Gorelick, N., Yadav, K., & Congalton, R. G. (2020). Mapping croplands of Europe, Middle East, Russia, and Central Asia using Landsat, Random Forest, and Google Earth Engine. *ISPRS Journal of Photogrammetry and Remote Sensing*, *167*, 104–122. https://doi.org/10.1016/J.ISPRSJPRS.2020.06.022

Piao, Y., Jeong, S., Park, S., & Lee, D. (2021). Analysis of Land Use and Land Cover Change Using Time-Series Data and Random Forest in North Korea. *Remote Sensing 2021, Vol. 13, Page 3501*, *13*(17), 3501. https://doi.org/10.3390/RS13173501

Priyono, K. D., Saifuddin, A., Nugroho, F. S., & Jumadi, J. (2022). Identification of Mangrove Changes in the Mahakam Delta in 2007-2017 Using Alos/Palsar and Landsat. *International Journal of GEOMATE*, *23*(96), 77–84. https://doi.org/10.21660/2022.96.3312

Qi, Z., Yeh, A. G. O., Li, X., & Lin, Z. (2012). A novel algorithm for land use and land cover classification using RADARSAT-2 polarimetric SAR data. *Remote Sensing of Environment*, *118*, 21–39. https://doi.org/10.1016/J.RSE.2011.11.001

Rufin, P., Bey, A., Picoli, M., & Meyfroidt, P. (2022). Large-area mapping of active cropland and short-term fallows in smallholder landscapes using PlanetScope data. *International Journal of Applied Earth Observation and Geoinformation*, *112*, 102937. https://doi.org/10.1016/J.JAG.2022.102937

Sarono, S., Kurniawan, R., Yahya Ahmad Karim, N., Zaky Hadibasyir, H., Nurul Fadhilla, M., Arif Trisnanto, M., & Hamonangan Sinaga, J. (2015). REMOTE SENSING AND GIS INTEGRATION FOR PADDY PRODUCTION ESTIMATION IN BALI PROVINCE, INDONESIA. *Proceedings of the 36th Asian Conference on Remote Sensing 2015*.

Sashikkumar, M. C., Selvam, S., Karthikeyan, N., Ramanamurthy, J., Venkatramanan, S., & Singaraja, C. (2017). Remote Sensing for Recognition and Monitoring of Vegetation Affected by Soil Properties. *JOURNAL GEOLOGICAL SOCIETY OF INDIA*, *90*, 609–615. https://doi.org/10.1007/s12594-017-0759-8

Sheykhmousa, M., Mahdianpari, M., Ghanbari, H., Mohammadimanesh, F., Ghamisi, P., & Homayouni, S. (2020). Support Vector Machine Versus Random Forest for Remote Sensing Image Classification: A Meta-Analysis and Systematic Review. *IEEE Journal of Selected Topics in Applied Earth Observations and Remote Sensing*, *13*, 6308–6325. https://doi.org/10.1109/JSTARS.2020.3026724

Singha, M., Dong, J., Zhang, G., & Xiao, X. (2019). High resolution paddy rice maps in cloud-prone Bangladesh and Northeast India using Sentinel-1 data. *Scientific Data 2019 6:1*, *6*(1), 1–10. https://doi.org/10.1038/s41597-019-0036-3

Susilo, B., & Harini, R. (2018). Spatial Analysis and Visualization of Geographic Access to Food in the Capital Area of Bulungan Regency, North Kalimantan Province. *Forum Geografi*, *32*(2), 146–155. https://doi.org/10.23917/FORGEO.V32I2.7070

Widiyanto, D. (2019). Local Food Potentials and Agroecology in Yogyakarta Special Province, Indonesia. *Forum Geografi*, *33*(1), 64–81. https://doi.org/10.23917/FORGEO.V33I1.7795